Enhanced magnetic orbital moment of ultrathin Co films on Ge(100)

P. Ryan, R. P. Winarski, D. J. Keavney, J. W. Freeland, and R. A. Rosenberg
Advanced Photon Source, Argonne National Laboratory, Argonne, Illinois 60439, USA

S. Park
Los Alamos National Laboratory, Los Alamos, New Mexico 87545, USA

C. M. Falco
Optical Sciences Center, University of Arizona, Tucson, Arizona 85721, USA

(Received 7 July 2003; revised manuscript received 27 October 2003; published 20 February 2004)

Electronic and magnetic studies of Co films grown on Ge(100) are presented using two sample systems; incremental *in situ* Co depositions and a pre-made Co wedge structure. Both a magnetically inactive region and a corresponding Co-Ge intermixed region form at the interface of both systems. The Co grows in a uniform manner beyond this Co-Ge region with ~ 2 Å perpendicular roughness. At low coverage of the *in situ* grown system, the Co exhibited an enhanced orbit to spin moment ratio, while, at higher Co coverages, we measured a total magnetic moment of 1.53 μ_B in agreement with previously published results of bcc Co grown on GaAs. The Co wedge indicated a constant but larger orbit-spin ratio along the wedge possibly due to the presence of an overlayer.

DOI: 10.1103/PhysRevB.69.054416 PACS number(s): 75.70.Ak, 73.20.−r

The opportunity of fully exploiting the potential of the ''spintronic'' phenomenon rests in the ability to understand, control, and ultimately engineer the required materials and associated devices.[1] Investigating the wide variety of simple ferromagnetic semiconductor structures is a crucial factor in pushing this arena forward. Interfacial roughness, intermixing, mismatch-induced strain, etc., all affect the structural, electronic, and magnetic characteristics of such systems, which in turn determine the ability to create and control spin current. Spin-based devices require both semiconductor and ferromagnetic abilities in order to control the degree of the electron spin. The creation of spin current may be initiated either by a semiconductor with intrinsic ferromagnetic behavior, such as GaMnAs, or by injecting ferromagnetic induced spin resolved current into a semiconductor.[1] Unfortunately, the spin injection is significantly damped at the interface where intermixing and roughness at such a boundary determines the interfacial scattering of the spin current.

The prototypical ferromagnetic/semiconductor system has been Fe/GaAs. The Co/Ge system is also of great interest as hcp Co has the largest magnetic anisotropic energy (MAE) of the ferromagnetic transition metals, and germanium has the ability to interface readily with silicon. Early studies of this system examined the formation of localized epitaxial Co germanides, specifically Co_5Ge_7 and $CoGe_2$ on Ge(111).[2] Typically such reactions took place at elevated temperatures. Room-temperature deposition studies on Ge(111) found that effectively ~ 3 monolayers of Ge were displaced from the substrate forming an intermixed region.[3] Studies investigating temperature-dependent magnetic characteristics inferred a nonmagnetic intermixed region of ~ 4.2 Å with reduced substrate temperatures ranging from 120 to 300 K. Cobalt has been reported to grow in a bcc metastable phase on GaAs(001) and (110) and Si(001).[4–8] In these cases, the major crystallographic axes of both substrate and bcc overlayer coincided.

Experiments reported here were performed at beamline 4IDC of the Advanced Photon Source. A circularly polarized undulator provided intense flux of $>96\%$ circularly polarized photons.[9] The online analysis chamber was equipped with *in situ* growth and surface preparation capabilities. Photoemission spectroscopy and low energy electron diffraction characterized the quality of the prepared surfaces. An *in situ* electromagnet supplied a controllable field to perform x-ray magnetic circular dichroism (XMCD) measurements; XMCD is the difference in the circularly polarized absorption spectra with alternating spin directions within the ferromagnetic sample. XMCD was measured via total electron yield with the sample in a remanent magnetic state. Sum rule analysis[10] of the XMCD data primarily measures the ratio of the orbit and spin magnetic moments (L/S).[11] The XMCD signal is treated to account for both the 45° angle offset between the applied field and the incident light and the 96% degree of polarization of the incident photons. To measure the orbit and spin moments independently, the electron occupancy of the $3d$ states is required. For the films at higher Co coverages, an averaged bulk reference is taken from previously published works.[12] In order to identify changes in the electron occupancy with different Co thickness, the absorption spectra may be integrated revealing the electron (hole) occupation of the $3d$ states as illustrated in Fig. 1(a), changes in ''r,'' the integrated absorption, at lower coverages may reveal charge transfer to or from the metal overlayer. To prepare the absorption spectra for integration, they were normalized with respect to the pre- and post-edges, shown in Fig. 1(a); a 2:1 stepped function was fit to the background regarding the respective quantum degeneracy $(2j+1)$ and removed, and the residual spectra was then integrated.

Once the XMCD data have been prepared several measurements are required in order to use sum rules. Figure 1(b) indicates the measurements of both p and q, which indicate the integrated measure across the L_3 edge alone and across

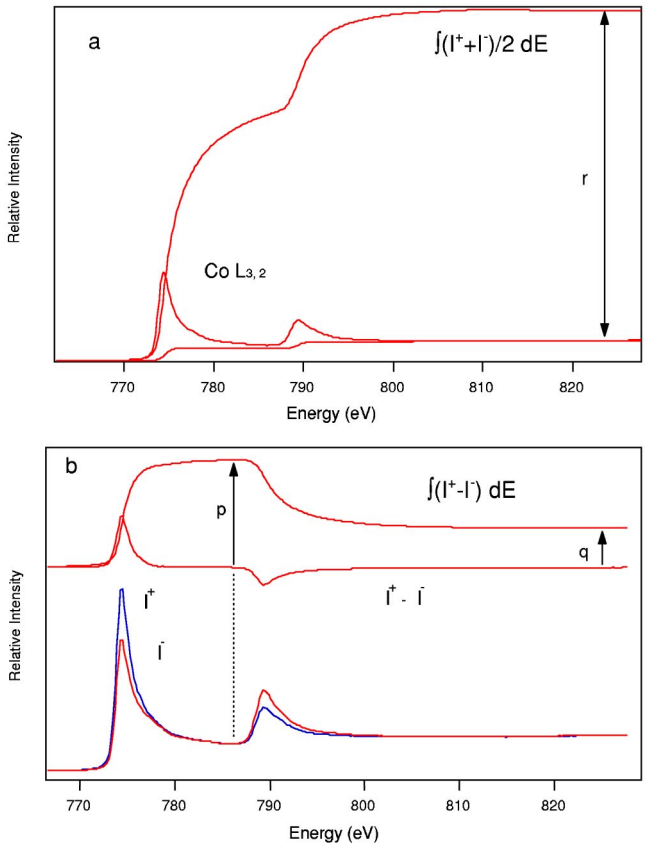

FIG. 1. (Color online) (a) The normalized Co $L_{3,2}$ absorption is first fit with a 2:1 stepped background; once removed, the integrated absorption quantity "r" may represent the hole count of the 3d states. (b) Absorption spectra with both antiparallel spin directions. The difference is the dichroic signal.

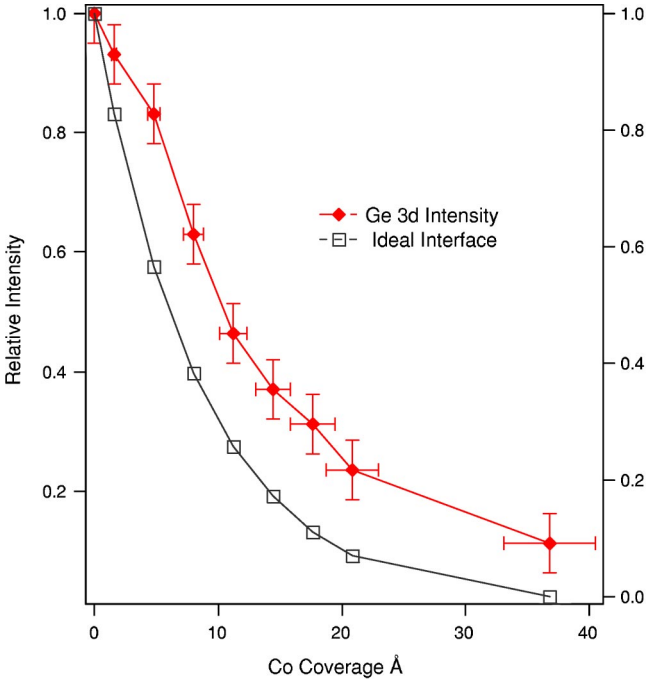

FIG. 2. (Color online) Ge 3d core level intensity decay plotted alongside calculated exponential decay with increasing Co deposition of sample 1. The displacement from the "ideal" decay path indicates Co-Ge intermixing.

both edges, respectively. In order to measure p, the minimum intensity between the absorption edges is selected and this position of the XMCD is used. The orbit-spin moment ratio is calculated as $2q/(9p\text{-}6q)$ and both the orbital and spin moments per atom can be calculated as $-4q(10\text{-}n_{3d})/3r$ and $-(6p\text{-}4q)(10\text{-}n_{3d})/r$, respectively.[11]

Soft x-ray scattering was used to measure the roughness of the film growth. The energy of the incident x rays was set at the Co L_3 edge, and the specularly reflected light was measured. The sample was then rotated (rocked) around the axis perpendicular to the detection plane as to scan across the specular and diffuse regions of the reflected beam. By analyzing the ratio of these regions and measuring the half width of the diffuse spectra, one can measure both perpendicular roughness and in-plane correlation lengths.[13] The nature of such reflectivity measurements makes this technique extremely surface/interface sensitive.

The incremental Co films were grown on the Ge(100) substrate (sample 1) which was cleaned and prepared *in situ* by Ar^+ sputtering and annealing, producing a clear and sharp (2×2) low energy electron diffraction (LEED) pattern with spot intensities alternating high and low, indicating two (2×1) domains oriented 90° from each other. Photoemission data showed no evidence of either C or O on the surface. Cobalt was deposited using e-beam evaporation from a Co rod, and the substrate was maintained at low temperature $\sim$170 K in order to try to minimize intermixing and avoid the formation of alloys. The evaporation rate was measured using a flux detector calibrated with a crystal monitor.

At 4.8 Å Co, the LEED pattern was gone and did not return with further deposition indicating long-range disorder at the surface. A similar loss of a diffraction pattern was reported for the Co/GaAs(001) system where transition electron microscopic results suggested that crystalline grains of $\sim$100 Å formed on the deposited Co surface,[14] but the film still indicated fourfold in-plane magnetic anisotropy, which suggests that epitaxy was preserved. Blundell *et al.*[7] also discussed the loss of LEED immediately after depositing a few Å Co on GaAs(001), but in this case, reflection high energy electron diffraction patterns persisted throughout the growth process.

The Co wedge (sample 2) was grown separately in order to gain easier access to a wider thickness range and to study temperature dependence. The Ge(100) surface was treated with an HCl based *ex situ* etch followed by *in situ* annealing at 640 °C.[15] The 0–50 Å Co wedge was grown at room temperature on the substrate taken from the same wafer as the previous sample and capped with a 30 Å Au protective layer. The sample was then removed from vacuum and transported to the beamline.

Figure 2 follows the photoemission intensity decay of the Ge 3d core level of sample 1, plotted alongside the calculated Ge 3d exponential decay. The immediate displacement from the "ideal" calculation indicates substrate disruption and an intermixed region of $<$4.8 Å. Published reports of

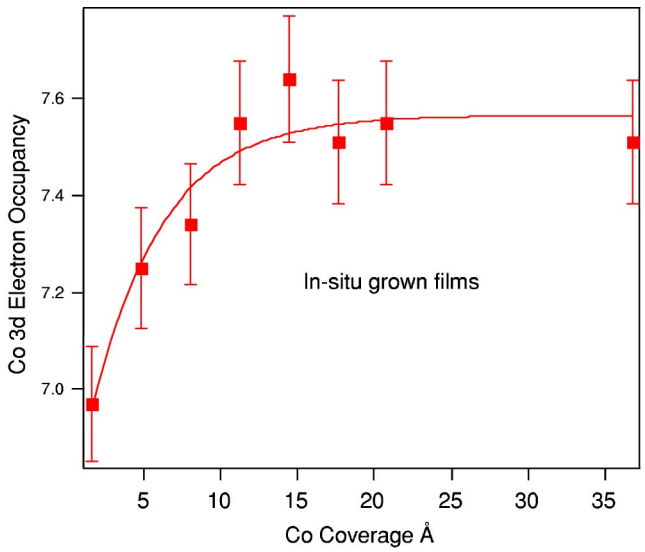

FIG. 3. (Color online) The electron occupancy of the Co 3*d* states vs Co coverage for sample 1. The fit exponential line is a guide for the eye.

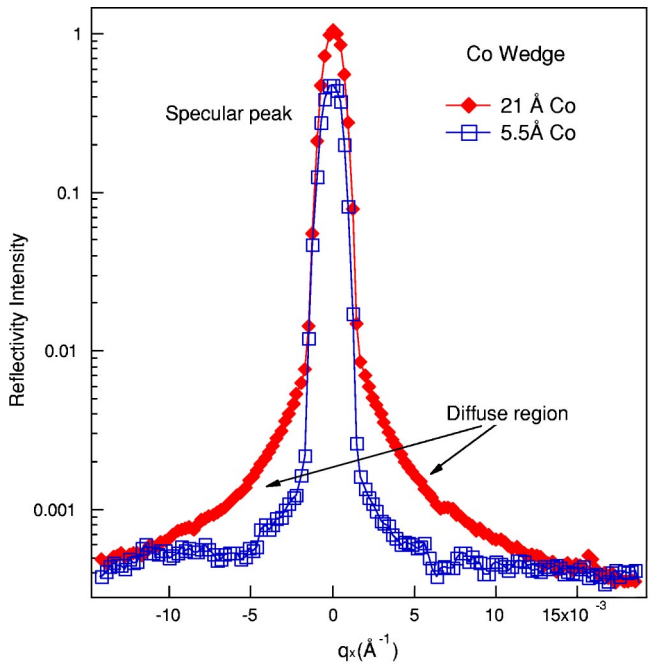

FIG. 4. (Color online) Soft x-ray rocking curves taken at the Co L_3 edge. Spectra of 21 and 5.5 Å are shown. The narrow width of the specular peak indicates very flat uniform growth. A qualitative roughness can be calculated by the ratio of the specular and diffuse spectral areas and indicates uniform growth of ~2 Å roughness along the wedge.

deposition at room temperature indicated ~4.2 Å Co-Ge interfacial mixing on the Ge(111) surface.[3] Evidently the low-temperature growth does not eliminate intermixing. Beyond this interfacial region, the decay path parallels that of the calculated intensity decay as the Co grows in a uniform manner upon the Co-Ge region.

The change in the electron occupancy of the Co 3*d* states is estimated by the normalization, background removal, and integration of the Co absorption $L_{3,2}$ intensities as illustrated in Fig. 1(a).[16] Figure 3 shows the 3*d* electron occupation of the *in situ* grown films as a function of Co film thickness. The final thick (36 Å) film was assigned a bulk value of 7.51 3*d* electrons per Co atom averaged from theoretical calculations.[11] A drop in occupancy is clear at the low coverage indicating a charge transfer into the substrate. Below this point, the signal-to-noise ratio was too small to measure the occupancy accurately. The relatively large difference between the electronegativities of Co (1.88) and Ge (2.01) might present a simple explanation of the charge transfer from Co. Similar results have been reported for Fe on GaAs, which was explained by the large difference in Fe and As electronegativities.[16]

An important factor in determining the quality of the thin-film growth is to understand its long-range morphology and film roughness. To investigate this, we analyzed soft x-ray reflectivity (scattering) based ''rocking curves'' taken along the wedge structure. These measurements examine the top few layers of the Co film giving quantitative measurements of the physical roughness of the Co growth.[13] Figure 4 shows two examples of rocking curves taken at 21 and 5.5 Å. The 21 Å plot is typical of the curves through most of the wedge (as low as 9.5 Å) giving a perpendicular roughness measurement (σ_p) of ~2 Å. At 7.5 Å and particularly at 5.5 Å a significant flattening of the diffuse spectra indicates a strong level of Co-Ge intermixing. The lack of significant diffuse scattering at 5.5 Å inhibits a reliable quantitative measure of the roughness, however, comparing the similarity between the two specular peaks we estimated that the roughness even at 5.5 Å is in the region of a few angstroms. The diffuse spectral shape broadens with increasing wedge thickness from 5.5 Å and stabilizes by 9.5 Å, indicating a deeper intermixed region with respect to the *in situ* grown sample.

Figure 5(a) shows the total Co L_3 XMCD signal of both the thin-film system and the wedge structure with different Co coverages. Below ~25 Å, for both systems, the signal drop is linear. The magnetic onset may be estimated by linear back extrapolation similar to remanance measurements using the magneto optic Kerr effect.[17] Thus 2.1 and 4 Å of nonmagnetic cobalt were identified for samples 1 and 2, respectively.

The inset in Fig. 5(a) shows a selected hysteresis loop at 14.4 Å Co of sample 1. If, as discussed, the (100) bcc Co direction coincides with the (100) Ge direction, the hysteresis loops were measured for sample 1 with the sweeping magnetic field applied close to the (110) Co direction. Sharp hysteresis loops with low coercivity through this system indicated high-quality film growth. Without azimuthal sample control, in-plane uniaxial anisotropy was not investigated as has been reported for the Co GaAs[7] and Fe Ge[18] systems. Double-stepped hysteresis loops reported for bcc Fe on Ge (100)[18] has been suggested to indicate in-plane uniaxial anisotropy, this behavior may be caused by the inequivalent in-plane (2×1) Ge surface reconstruction described by Ma and Norton.[18] The $2\times(2\times1)$-90° surface reconstruction identified here would screen any such effect. It is also noted that for sample 1 the field was applied close to the diagonal of both (2×1) surface reconstruction domains, thus the

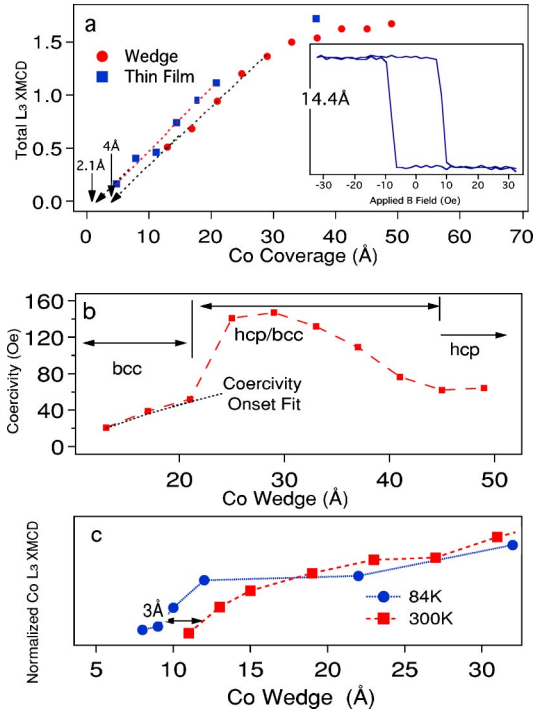

FIG. 5. (Color online) (a) Plot of XMCD signal vs Co coverage of both samples. The inset shows a soft x-ray hysteresis loop at the Co L_3 edge at 14.4 Å. Back extrapolation estimates the magnetic onset. (b) Coercivity measurements are plotted along the wedge. Three phases are inferred from the changes in coercivity. (c) Normalized XMCD signal plotted along the wedge at both 84 and 300 K. A change in T_C of the Co film shifts the magnetic onset between the two spectra.

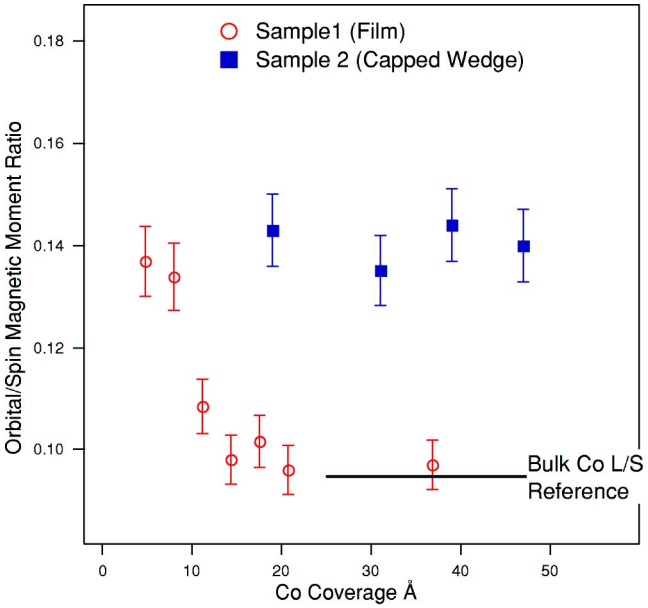

FIG. 6. (Color online) The ratio of orbit to spin magnetic moments calculated from the sum rules analysis of XMCD data for both sample systems. An increase in the ratio at low Co coverage of sample 1 indicates an enhanced orbital contribution to the magnetic moment. The increase in L/S along the Co wedge is due most likely to the presence of an overlayer.

stepped loop affect may not be discernible. For the wedge structure the field was applied along the (100) bcc Co direction and here no evidence of stepped loops was detected either. The hysteresis loops were also not as square as for the *in situ* grown sample, and the coercivity was slightly larger even though the (100) Co direction is expected to be the easy magnetic axis. This could be caused by the greater extent of intermixing at the wedge interface due to the higher substrate temperature (300 K) during Co deposition.

Figure 5(b) shows the coercivity of the hysteresis loops along the Co wedge. The onset has been fit with a power law $Hc \sim (d/dc\text{-}1)^{\alpha}$, where d is the Co thickness, dc is the onset thickness (4 Å) and using $\alpha = 0.58$ as calculated for the growth of Co on Cu(100). There is good agreement up to $\sim$21 Å. Although this empirical fit indicates the coercivity increase to be the result of a thermodynamic dependence,[19] more importantly it highlights the sudden change beyond $\sim$21 Å. The coercivity dramatically increases to a maximum at $\sim$30 Å and in turn falls until $\sim$45 Å, where it stabilizes. These changes are attributed to a structural transition from bcc to the more relaxed bulk hcp phase, seen previously in thin Co films.[5,8] In a very similar fashion, reflection high energy electron diffraction patterns of Co growth on GaAs (001)[5] reported bcc growth up to 20 Å; with further Co deposition, hcp begins to form, coexisting with the bcc phase, which gradually disappears and is gone entirely by 60 Å Co.

Figure 5(c) shows the L_3 XMCD signal along the wedge structure at both 84 and 300 K, illustrating an onset shift of the magnetic signal $\sim$3 Å between the two temperatures. Ultrathin ferromagnetic films experience a decrease in Curie temperature (T_C) as described by finite-size scaling theory. Several factors, such as magnetic anisotropy, exchange coupling, and electronic band structure, change with a transition from bulk to atomic scale thin films as the perpendicular symmetry is broken. This region is estimated to range between 8 and 11 Å. The rocking curves indicate that the intermixed region extends to at least 7.5 Å; beyond this point, the Co forms the two-dimensional structure with reduced symmetry, which agrees with the onset of a reduced T_C region.

Magnetocrystalline anisotropic energy (MAE) forces the magnetization to align in specific orientations. The structure and thus the symmetry of the material affect the MAE. This orientation-related energy is mediated by the orbital magnetization through the spin-orbit interaction, which links the spin to the atomic structure of the ferromagnet.[20] For both Co systems under investigation, in-plane anisotropy has been identified where no out of plane XMCD signal was measured, coupling this with the lack of uniaxial in-plane anisotropy we endeavor to obtain an understanding about the in-plane orbital moments.

Sum rule analysis of the XMCD spectra measures the ratio between the orbit to spin contributions (L/S) to the magnetic moment of the Co overlayer. The in-plane L/S ratios are plotted for both samples in Fig. 6, and the bulk Co reference was taken from published results of hcp Co also measured by XMCD although in transmission.[11] The L/S ratio of Co film above 15 Å in sample 1 aligns well with this

TABLE I. Orbital and spin magnetic moments (M_L,M_S), their ratios (L/S), and the total moments (M_T) both from sample 1 (36 Å) and sample 2 (averaged from 30 to 50 Å), taking into consideration the nonmagnetic interfacial Co.

Sample	L/S	M_L μ_B	M_S μ_B	M_T μ_B
In situ grown: 36 Å sample 1	0.097	0.14	1.44	1.53
Co wedge (30–50 Å) sample 2	0.14	0.22	1.7	2
Co hcp bulk[a]	0.095	0.154	1.62	1.774

[a]Bulk XMCD reference taken from Chen *et al.* (Ref. 11).

reference figure. An enhanced ratio was measured at lower coverages (4.8–8 Å). Here the ultrathin film structure reduces the Co symmetry as seen by an orbital magnetic moment increase; the spin contribution should remain unaffected resulting in an increase of the L/S ratio.

Such orbital enhancement has been debated for fabricated Co structures. The Co orbital moment within Co(250 Å)/Pd multilayers was reported to show an increase from 0.17 μ_B to 0.24 μ_B moment per atom, and more recently large increases in the orbital moment of Co nanodots on Pt(111) have been measured where there is a large reduction in symmetry.[20]

Figure 6 also shows the L/S ratio for the capped Co wedge (sample 2) showing a relatively constant but enhanced ratio across the wedge. Applying the full sum rule analysis, the orbital moment was also uniform across the wedge beyond the effect of the nonmagnetic interface, an averaged orbital moment across this portion of the wedge (30–50 Å) measured 0.22 μ_B (Table I). This indicates a significant increase of 57% from the *in situ* grown 36 Å film (0.14 μ_B). This enhancement is similar to the 59% orbital increase of the Co/Pd system.[20] It is perhaps evident that an overlayer affects the Co orbital moment by altering the film orbital symmetry. The wedge structure also shows an increased bulk total moment of 2 μ_B, with respect to 1.53 μ_B of bulk Co. While the spin moment increase is relatively small ~15% with respect to the 36 Å Co film, the orbital increase of 57% is considerably greater. This illustrates the strong symmetry effect on the orbital moment. It is been reported that overlayers have been used to induce and modify perpendicular anisotropy within Co thin films,[21] and more detailed studies are being pursued to study the effects different over and underlayer wedges of Cu and Au will have on the magnetic characteristics of varying thicknesses of Co films.

The total moment reference for hcp Co is quoted as 1.714 μ_B,[22] very close to the XMCD measurements by Chen *et al.* of 1.774 μ_B.[11] Prinz[8] on the other hand measured an averaged magnetic moment of 1.53 μ_B for thin Co films on GaAs, using the known bcc Co lattice constant. Bland *et al.* similarly reported a reduced moment 1.4 μ_B for bcc Co on GaAs.[6] Taking into account the nonmagnetic layer (2.1 Å) for the *in situ* grown thin-film sample, a total magnetic moment of 1.53 μ_B (at 36 Å, Table I) agrees well with the reduced moments of both Prinz[8] and Bland *et al.*[6]

In summary, the growth, electronic structure, and magnetic characteristics of epitaxial Co on Ge(100) have been investigated, for both *in situ* grown samples and a Au capped wedge structure. Photoemission data indicated the formation of a <4.8 Å Co-Ge mixed interfacial region for the *in situ* grown sample. Rocking curves of the Co wedge system presented evidence of a similar but larger intermixed region ~7.5 Å. The Co thickness magnetic onsets were estimated at 2.1 and 4 Å for the *in situ* and wedge samples, respectively. Coercivity measurements along the wedge showed a dramatic change due to a bcc to hcp phase transition similar to that found in the Co/GaAs(100) system. The growth of Co beyond the Co-Ge intermixed region from both the photoemission intensity decay and rocking curves is uniform, with the wedge showing a typical perpendicular roughness of ~2 Å.

XMCD indicated an enhanced orbital moment for a narrow region of Co growth above the Co-Ge interfacial region for the *in situ* grown sample, where a loss of perpendicular symmetry enhances the orbital moment. The total moment per atom was then measured at 1.53 μ_B (at 36 Å) comparing well with Prinz[8] and Bland *et al.*[6] for thin Co films on GaAs of 1.53 μ_B and 1.4 μ_B, respectively. All these are lower than the hcp Co reference of 1.714 μ_B (Ref. 22) and 1.774 μ_B by Chen *et al.*[11]

Use of the APS was supported by the U.S. Department of Energy, Office of Science, Office of Basic Energy Sciences, under Contract No. W-31-109-ENG-38. Work at the University of Arizona was supported by the U.S. Department of Energy under Grant No. DE-FG03-93ER45488.

[1] G. A. Prinz, Phys. Today **48** (4), 58 (1995).
[2] Y. F. Hsieh, L. J. Chen, E. D. Marshall, and S. S. Lau, Appl. Phys. Lett. **51**, 1588 (1987).
[3] G. A. Smith, L. Luo, S. Hashimoto, and W. M. Gibson, J. Vac. Sci. Technol. A **7** , 1475 (1989).
[4] F. Xu, J. J. Joyce, M. W. Ruckman, H. W. Chen, F. Boscherini, D. M. Hill, S. A. Chambers, and J. H. Weaver, Phys. Rev. B **35**, 2375 (1987).
[5] Y. Z. Wu, H. F. Ding, C. Jing, D. Wu, G. L. Liu, V. Gordon, G. S. Dong, and X. F. Jin, Phys. Rev. B **57**, 11935 (1998).
[6] J. A. C. Bland, R. D. Baterson, P. C. Riede, R. G. Graham, H. J. Lauter, J. Penfold, and C. Shackleton, J. Appl. Phys. **69**, 4989 (1991).
[7] S. J. Blundell, M. Gester, J. A. C. Bland, C. Daboo, E. Gu, M. J. Baird, and A. J. R. Ives, J. Appl. Phys. **73**, 5948 (1991).
[8] G. A. Prinz, Phys. Rev. Lett. **54**, 1051 (1985).
[9] J. W. Freeland, J. C. Lang, G. Srajer, R. Winarski, D. Shu, and D. M. Mills, Rev. Sci. Instrum. **73**, 1408 (2002).
[10] B. T. Thole, P. Carra, F. Sette, and G. v. d. Laan, Phys. Rev. Lett. **68**, 1943 (1992).

[11] C. T. Chen, Y. U. Idzerda, H.-J. Lin, N. V. Smith, G. Meigs, E. Chaban, G. H. Ho, E. Pellegrin, and F. Sette, Phys. Rev. Lett. **75**, 152 (1995).
[12] W. C. Cheng, J. S. Tsay, Y. D. Yao, K. C. Lin, C. S. Yang, S. F. Lee, T. K. Tseng, and H. Y. Neih, J. Appl. Phys. **89**, 7130 (2001).
[13] J. W. Freeland, K. Bussman, Y. U. Idzerda, and C.-C. Kao, Phys. Rev. B **60**, R9923 (1999).
[14] E. Gu, R. J. Hicken, C. Daboo, M. Tselepi, S. J. Gray, J. A. C. Bland, and L. M. Brown, Phys. Rev. B **52**, 14704 (1995).
[15] P. Etienne, J. Cryst. Growth **111**, 1003 (1991).
[16] J. W. Freeland, I. Coulthard, J. W. J. Antel, and A. P. J. Stampfl, Phys. Rev. B **63**, 193301 (2000).
[17] Y. B. Xu, E. T. Kernohan, D. J. Freeland, A. Ercole, M. Tselepi, and J. A. C. Bland, Phys. Rev. B **58**, 890 (1998).
[18] P. Ma and P. R. Norton, Phys. Rev. B **56**, 9881 (1997).
[19] F. O. Schumann and J. A. C. Bland, J. Appl. Phys. **73**, 5945 (1993).
[20] P. Gambardella, S. Rusponi, M. Veronese, S. S. Dhesi, C. Grazioli, A. Dallmeyer, I. Cabria, R. Zeller, P. H. Dedrichs, K. Kern, C. Carbone, and H. Brune, Science **300**, 1130 (2003).
[21] S. Park, S. Lee, and C. M. Falco, J. Appl. Phys. **91**, 8141 (2002).
[22] R. M. Bozorth, *Ferromagnetism* (Van Nostrand, Reinhold, New York, 1951).